

Synthesis and Characterization of Oxide Feedstock for the Fuel Cycle R&D, Advanced Fuels Campaign – Fiscal Year 2010

Stewart Voit, Ray Vedder, Jared Johnson
Oak Ridge National Laboratory

1. Introduction

Nuclear fuel feedstock properties, such as physical, chemical, and isotopic characteristics, have a significant impact on the fuel fabrication processⁱ and, by extension, the in-reactor fuel performance.ⁱⁱ This has been demonstrated through studies with UO₂ spanning greater than 50 years.^{iii,iv}

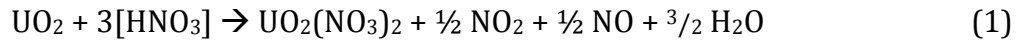
The Fuel Cycle R&D Program with The Department of Energy Office of Nuclear Energy has initiated an effort to develop a better understanding of the relationships between oxide feedstock, fresh fuel properties, and in-reactor fuel performance for advanced mixed oxide compositions. Powder conditioning studies to enable the use of less than ideal powders for ceramic fuel pellet processing are ongoing at Los Alamos National Laboratory (LANL) and an understanding of methods to increase the green density and homogeneity of pressed pellets has been gained for certain powders. Furthermore, Oak Ridge National Laboratory (ORNL) is developing methods for the co-conversion of mixed oxides along with techniques to analyze the degree of mixing.

Experience with the fabrication of fuel pellets using co-synthesized multi-constituent materials is limited.^v In instances where atomically mixed solid solutions of two or more species are needed, traditional ceramic processing methods have been employed. Solution-based processes may be considered viable synthesis options^{vi}, including co-precipitation (AUPuC), direct precipitation, direct-conversion (Modified Direct Denitration or MDD) and internal/external gelation (sol-gel). Each of these techniques has various advantages and disadvantages.

The Fiscal Year 2010 feedstock development work at ORNL focused on the synthesis and characterization of one batch of UO_x and one batch of U₈₀Ce₂₀O_x. Oxide material synthesized at ORNL is being shipped to LANL for fuel fabrication process development studies. The feedstock preparation was performed using the MDD process which utilizes a rotary kiln to continuously thermally denitrate double salts of ammonium and metals to produce free-flowing powders that have good ceramic properties for fuel fabrication.^{vii} Feedstock powder properties of interest include: particle size and distribution, surface area, phase purity, morphology, tap and bulk density, and flow characteristics.

2. Direct Conversion Process

The MDD equipment used in the FY10 work is setup in Building 7930 of the Radiochemical Engineering Development Center at ORNL. The MDD process starts with the dissolution of UO_2 in nitric acid to form a uranyl nitrate solution. The reaction shown in equation 1.



The dissolvent is preheated to 60°C to avoid a prolonged induction period followed by vigorous reaction. It is desirable to avoid excess nitric acid in the feed solution so the density of $\text{UO}_2(\text{NO}_3)_2 \cdot \text{HNO}_3$ was used in equation 1 to establish the appropriate acid concentration. Ammonium nitrate (NH_4NO_3) is added to the $[\text{UO}_2(\text{NO}_3)_z]$ solution to yield an NH_4/U ratio typically in the range of 2 to 2.6 mol:mol.

The feed solution is loaded into a graduated cylinder in preparation for delivery to the MDD heated kiln. The feed transfer operation is performed in a fume hood as shown in Figure 1.

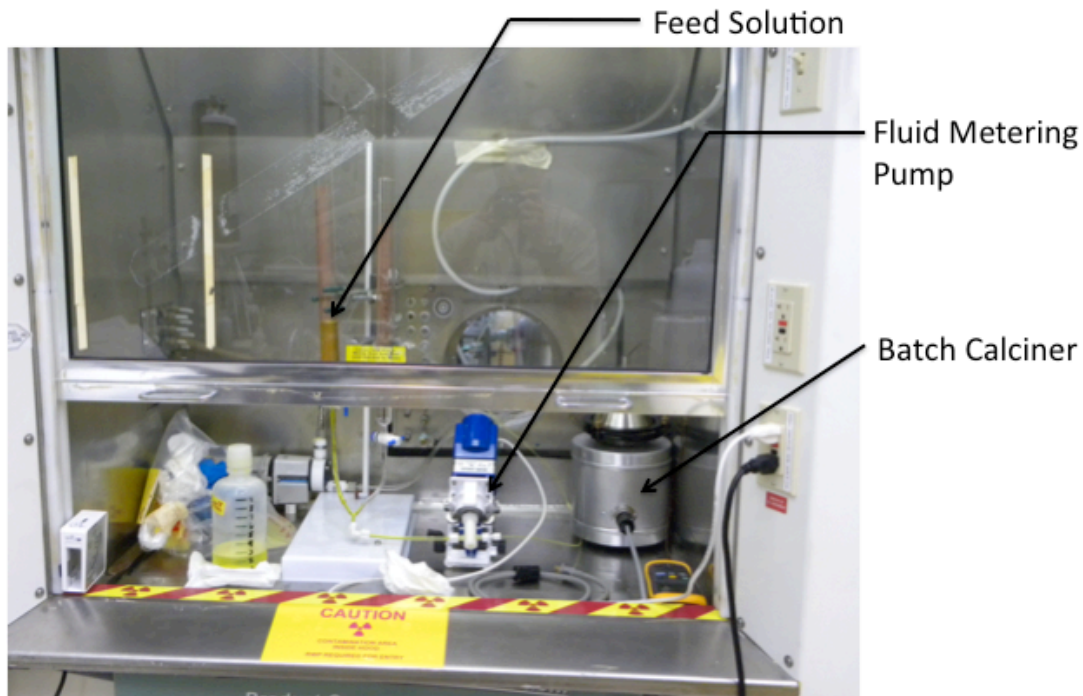


Fig. 1. Feed solution metering system.

The feed solution is transferred to the MDD kiln using a fluid metering pump. The kiln consists of a center drip tube which is surrounded by a rotating three zone heated chamber (see Figure 2). The center tube and heated chamber are inclined at a slope of ~ 6 degrees to allow gravity induced flow of material. Feed solution is

injected into the region of the first heat zone and decomposition takes place as a function of time and temperature.

The ammonium nitrate-uranyl nitrate double salt, $(\text{NH}_4)_2\text{UO}_2(\text{NO}_3)_4$, begins to dehydrate at 50°C followed by anhydrous tetranitrate decomposition at $170\text{-}270^\circ\text{C}$ forming a trinitrate salt. The trinitrate decomposes at $270\text{-}300^\circ\text{C}$ to form an amorphous metal trioxide (MO_3). The net effect is that the MDD process converts the feed solution directly to the solid state (without melting) and yielding large soft agglomerates of fine grain oxide particles.

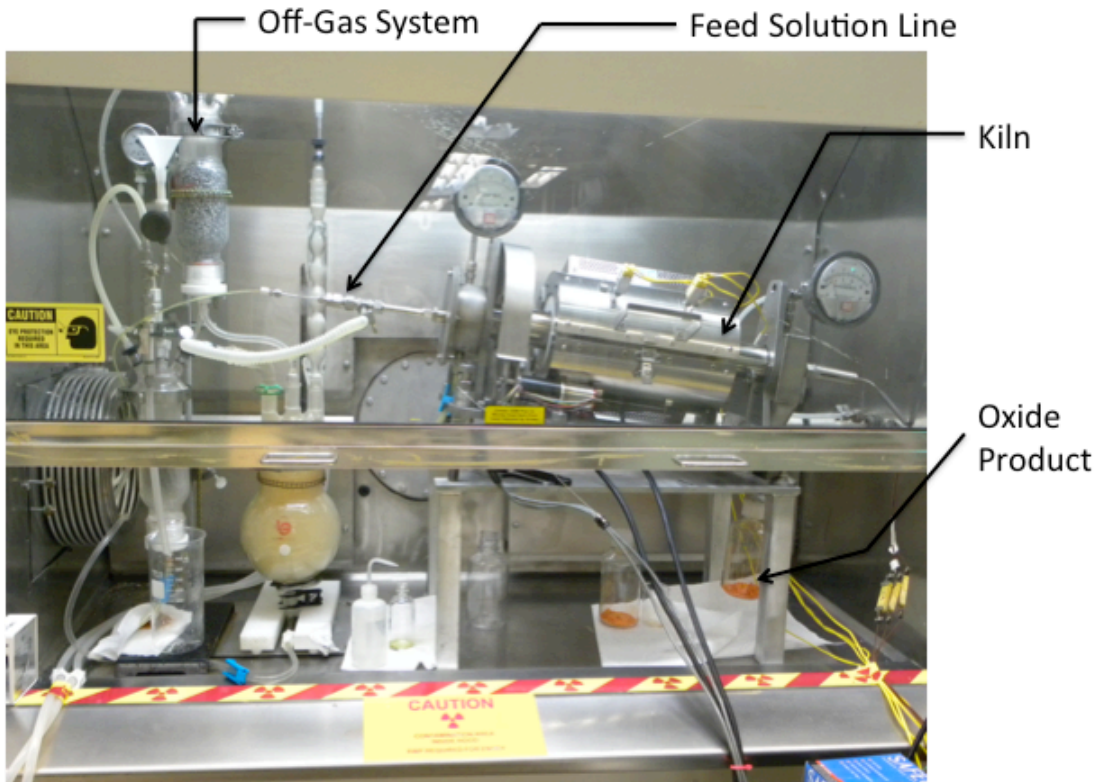


Fig. 2. MDD kiln and off-gas system.

Figure 3 is a cross-sectional drawing of the kiln configuration showing the approximate temperature profile. The diagram in Figure 3 makes reference to two roller bars that are used to remove material from the walls of the chamber as it rotates. The actual system shown in Figure 2 has been modified to replace the roller rods with scraper bars that are fixed to the center tube. The scraper bars perform the same function as the roller rods, however the new design is expected to eliminate the problem of the roller rods becoming bound as the furnace rotates.

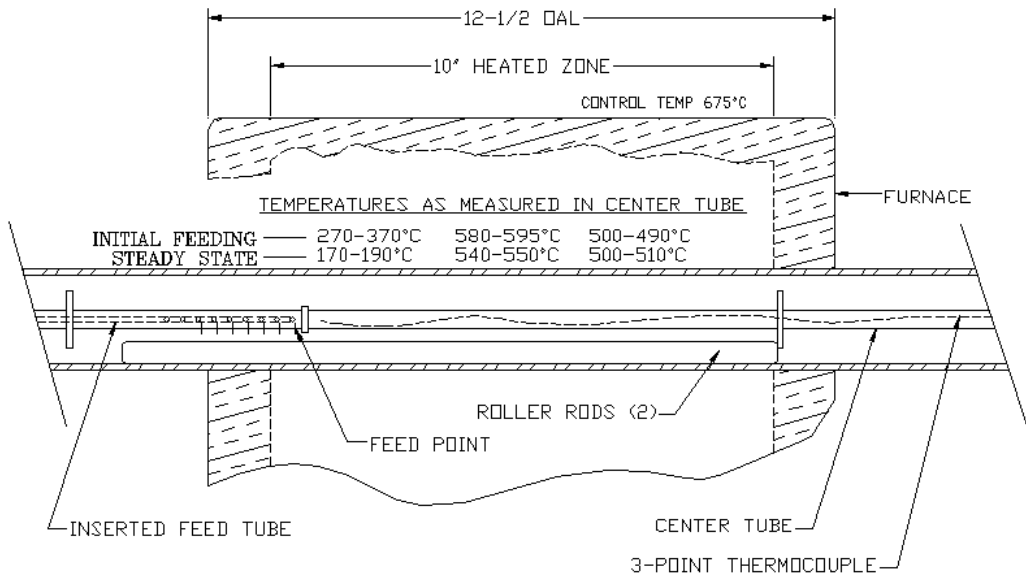


Fig. 3. Cross-sectional drawing of kiln with temperature profile.

3. Direct Conversion to UO_x

The first batch of MDD produced oxide was performed using ABB UO_2 (ABB Atom AB Sweden) powder that was shipped to ORNL from LANL. ABB was selected for use because of its use as the historical baseline powder for fuel development activities at LANL. The ABB powder has a known pedigree with regards to impurities, isotopic vector, and particle characteristics.

The ABB UO_2 was dissolved in nitric acid using the method described in Section 2. The final concentration was ~ 330 gU/L, and 2 mol NH_4 per mol of U. Using an established correlation^{viii} on the effects of HNO_3 concentrations, the solution as determined to be approximately neutral. Processing of the feed solution proceeded as expected and approximately 148 grams of UO_3 powder was produced.

The oxide from the first run was calcined at $\sim 300^\circ C$ for approximately 1 hour. After calcining, the powder was sieved to -45 mesh (354 μm). The UO_3 product is amorphous so the powder was calcined at $\sim 525^\circ C$ and an X-ray Diffraction (XRD) pattern is shown in Figure 4. XRD results were obtained using a Rigaku Mini Flex-II x-ray diffractometer. The XRD results indicate that at $525^\circ C$, conversion to U_3O_8 is incomplete. This result is consistent with that of Hoekstra and Siegel^{ix} who show that $\beta-UO_3$ begins to decompose from the 3.0 U:O ratio at $530^\circ C$, but does not completely convert to the 2.67 U:O ratio of U_3O_8 until about $650^\circ C$.

Surface area measurements were performed using the Brunauer, Emmett, Teller (B.E.T) method using a Belorp-Mini surface area analyzer. The adsorption isotherm data points are plotted as a straight line as shown in Figure 5.

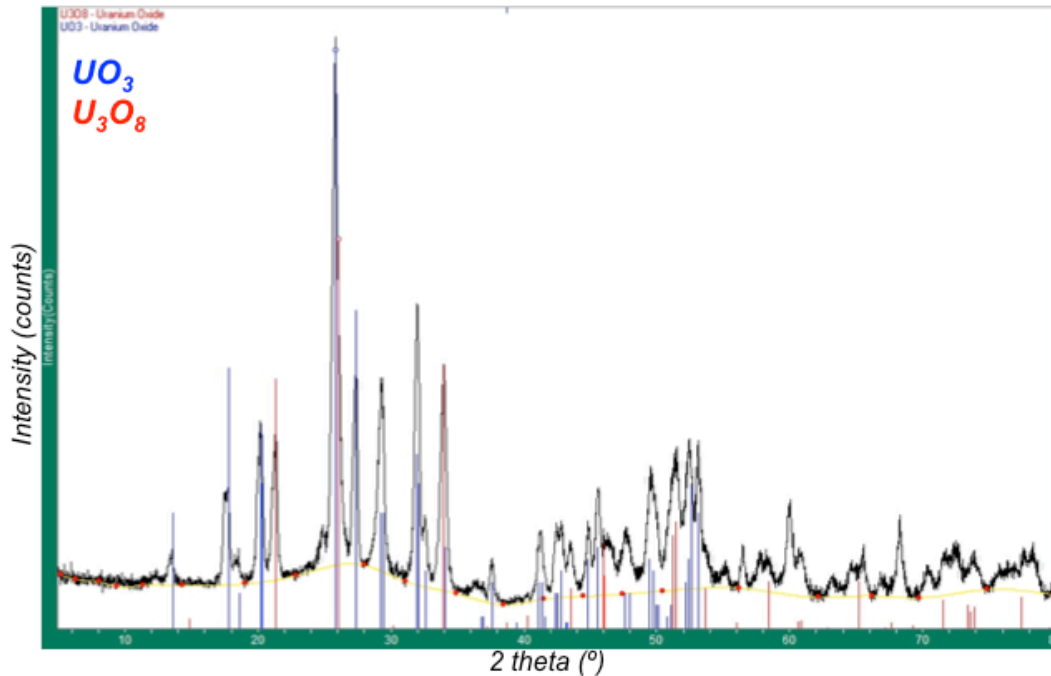


Fig. 4. XRD pattern of UO_3 powder calcined at $\sim 300^\circ\text{C}$.

Measurements were made with three samples taken from the calcined (at $\sim 300^\circ\text{C}$) and sieved (-45 mesh) product from the first MDD run. The samples were heated to 300°C for 1- $\frac{1}{2}$ hours as part of the Belorp-Mini sample conditioning routine. As can be seen in Figure 5, there was little variation between sample results indicating a uniform surface area across the batch. The B.E.T. specific surface areas were measured as: 7.1, 7.0, and 7.1 m^2/g . The B.E.T. constants were all above 100.

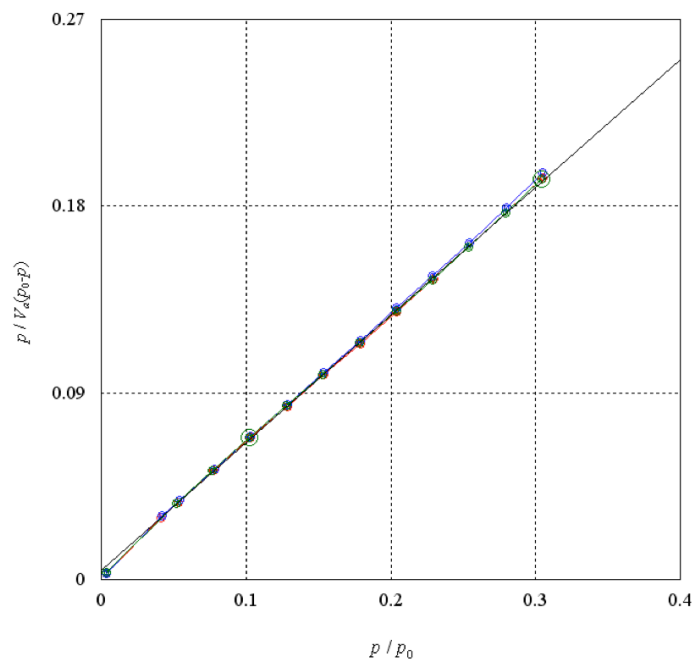
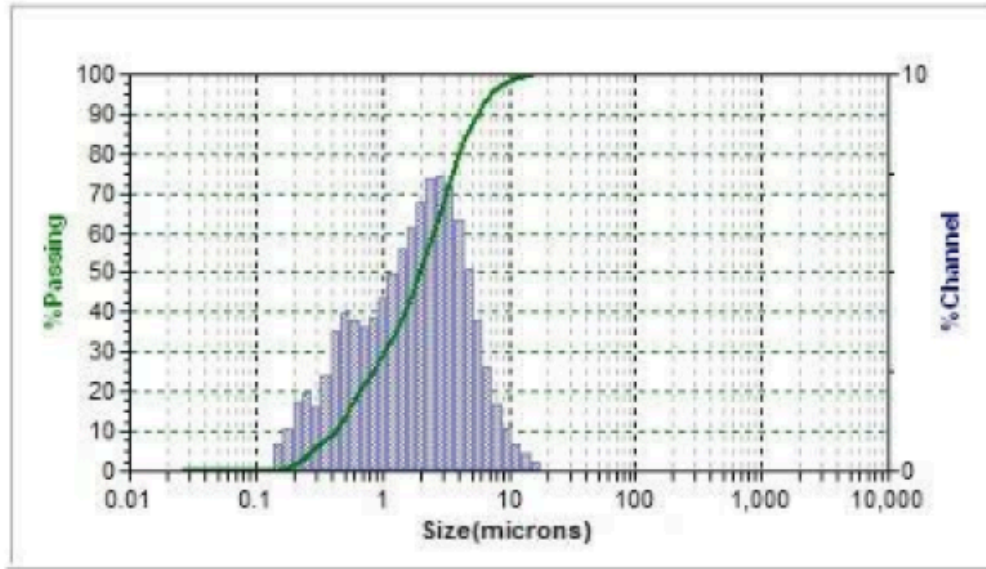


Fig. 5. B.E.T. surface area results for three UO_3 samples.

The particle size distribution (PSD) was measured with a Microtrac S3500 light scattering particle size analyzer. Samples were prepared by dispersing the calcined oxide in a dilute trisodium phosphate/water solution using a low energy ultrasonic probe. The result, which is the average of three consecutive runs, is presented in Figure 6.



Summary		Size Percent		Percentiles		Peaks		
Data Item	Value	Size(um)	%Tile	%Tile	Size(um)	Dia(um)	Vol%	Width
MV(um):	2.629			10.00	0.421	2.451	83.0	3.92
MN(um):	0.2790			20.00	0.662	0.448	11.6	0.18
MA(um):	1.031			30.00	1.044	0.2270	5.4	0.09
C S:	5.82			40.00	1.484			
SD:	2.008			50.00	1.981			
				60.00	2.539			
Mz:	2.369			70.00	3.20	UDef Name	UDef Data	
σ:	2.064			80.00	4.09			
Ski:	0.401			90.00	5.61			
Kg:	1.036			95.00	7.27			

Fig. 6. Particle size distribution for UO₃ samples.

The predominantly normal distribution shown in Figure 6 displays a slight hump on the submicron side of the profile. The distribution mean of 2.629 μm is expected to increase when the powder is reduced to the dioxide (UO₂) at LANL.

4. Direct Conversion to UCeO_x

The target composition for the second MDD run was $\text{U}_{1-y}\text{Ce}_y\text{O}_3$, where $y = 0.20$, and compound stoichiometry was achieved by dissolving the appropriate molar amount of cerium nitrate in the uranyl nitrate solution. The UCeO_x product powder was calcined at $\sim 300^\circ\text{C}$ then sieved to -45 mesh. XRD results of this intermediate product are inconclusive. The library of diffraction patterns is limited with respect to urania-ceria compounds and interpretation of the fit to known patterns is difficult because of overlapping peak positions for urania and ceria of varied oxygen stoichiometries.

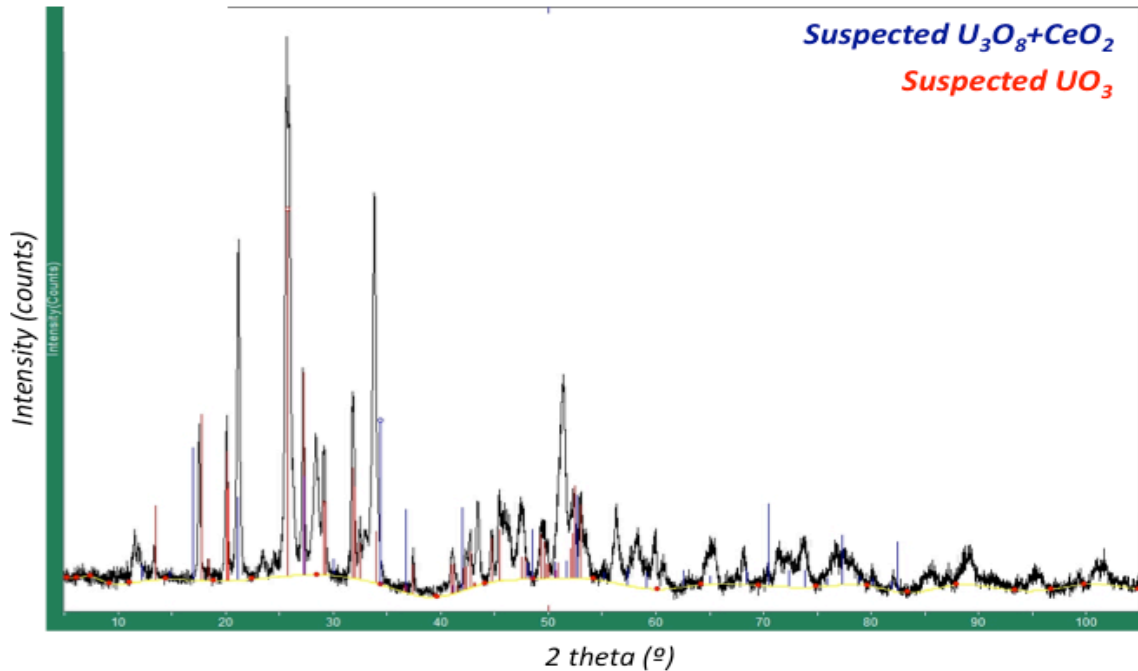


Fig. 7. XRD pattern of $\text{U}_{0.8}\text{Ce}_{0.2}\text{O}_3$ powder calcined at $\sim 300^\circ\text{C}$.

After calcination, an attempt was made to reduce a sample of the UCeO_x powder to UCeO_2 in a sealed furnace at $\sim 750^\circ\text{C}$ under flowing Ar-4\%H_2 for ~ 1 hour. The XRD result is displayed in Figure 8. Shown in Figure 9 is the diffraction pattern for $\text{U}_{0.79}\text{Ce}_{0.21}\text{O}_2$ from the Inorganic Crystal Structure Database (ICSD). As with the XRD result for the calcined sample (Figure 4), it appears that the stoichiometry adjustment was incomplete. The five peak positions, (1,1,1), (2,0,0), etc. in Figure 9 line up well with the major peaks from the sample shown in Figure 8, however, there are clearly unaccounted for peaks. Possible matches for these peaks can be found in the patterns for U_3O_8 and CeO_2 which would be consistent with the suggestion that the reduction was incomplete. Conclusions will not be made regarding the phase content of the calcined and reduced UO_x , and UCeO_x until the data undergoes Rietveld refinement.

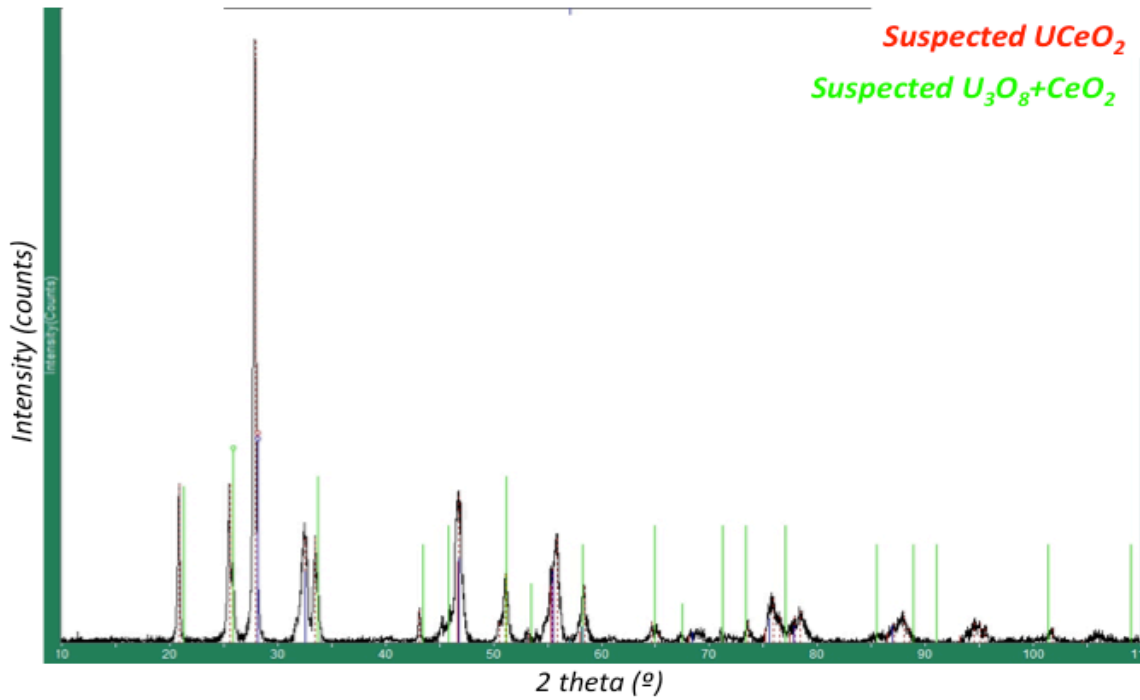


Fig. 8. XRD pattern of $U_{0.8}Ce_{0.2}O_2$ powder reduced at $\sim 750^\circ C$.

*-Ce.21 U.79 O2-[FM3-M]Ruedorff, W.; Valet, G.[1953]

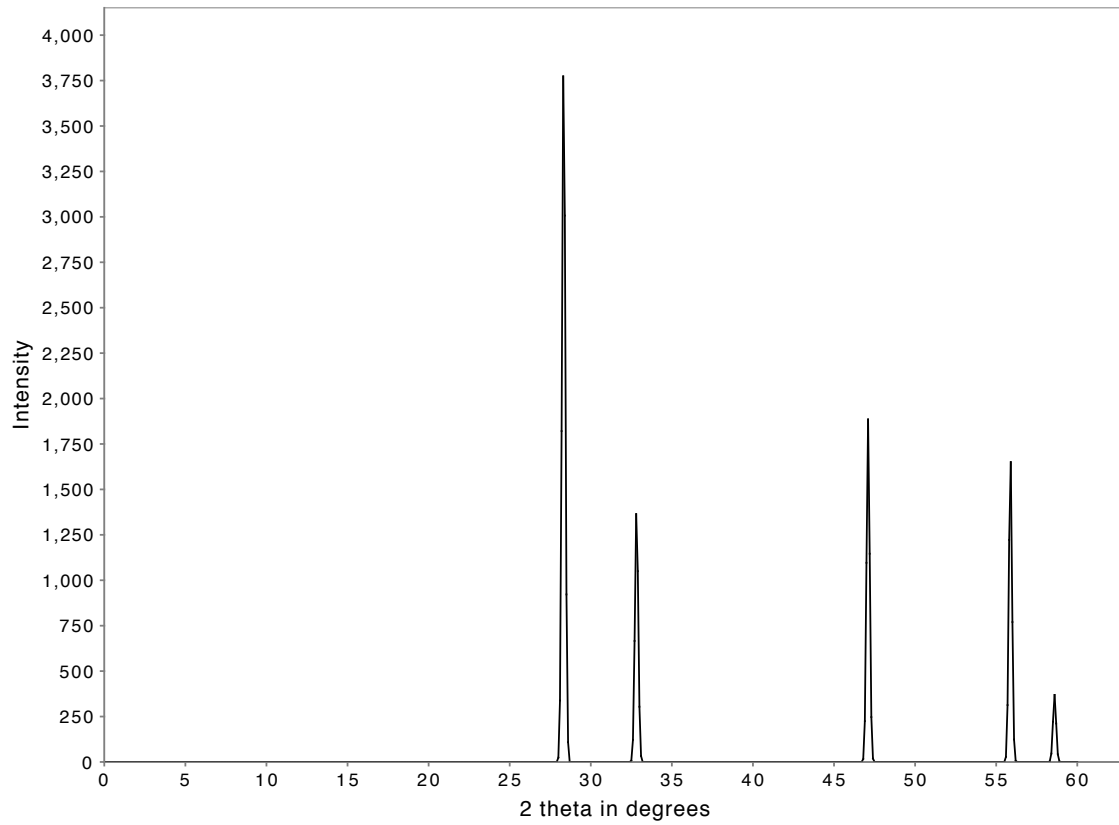
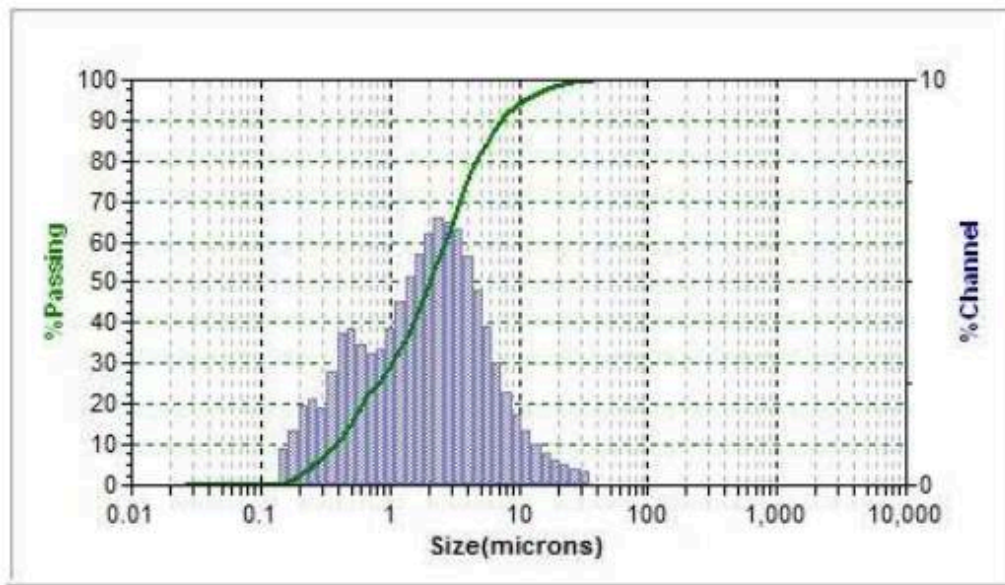


Fig. 9. XRD pattern of $U_{0.79}Ce_{0.21}O_2$ from ICSD.

Samples for the $U_{0.8}Ce_{0.2}O_3$ PSD were prepared using the method described in Section 3 for UO_x . The result, which is the average of three consecutive runs, is presented in Figure 10.



Summary		Size Percent		Percentiles		Peaks		
Data Item	Value	Size(um)	%Tile	%Tile	Size(um)	Dia(um)	Vol%	Width
MV(um):	3.35			10.00	0.386	2.773	77.9	5.16
MN(um):	0.2650			20.00	0.617	0.410	22.1	0.35
MA(um):	1.002			30.00	1.033			
CS:	5.99			40.00	1.519			
SD:	2.489			50.00	2.062			
				60.00	2.697			
Mz:	2.689			70.00	3.53	UDef Name	UDef Data	
σ:	2.870			80.00	4.75			
Ski:	0.521			90.00	7.32			
Kg:	1.352			95.00	10.99			

Fig. 10. Particle size distribution for $U_{0.8}Ce_{0.2}O_3$ samples.

As with the urania sample, the predominantly normal distribution shown in Figure 10 displays a slight hump on the submicron side of the profile. The distribution mean of 3.35 μm is effectively the same as the mean particle size for the first run with UO_x .

5. Conclusion

Synthesis of two urania-based compositions using MDD is complete. The product powder has been packaged and is being shipped to LANL for use in fuel fabrication

process development studies. Some characterization has been performed on the intermediate oxide product and in Fiscal Year 2011, the remaining UO_x and $UCeO_x$ will be fully reduced to the dioxide followed by a comprehensive characterization effort including:

- Phase purity (XRD and SEM)
- Particle size distribution (Laser diffractometry)
- Surface area (B.E.T.)
- Morphology (SEM)
- Bulk and tap density (per ASTM standard)
- Flowability (Powder rheometer)

Characterization of the dioxide powder from the first two runs will establish the baseline from which results of future MDD process development studies and the synthesis of additional compositions will be compared. A comparison will also be made with oxide feedstock particle characteristics from historical MDD work as well as powder from traditional ammonium diuranate (ADU), ammonium uranyl carbonate (AUC), and other powder from other synthesis methods.

ⁱ Vollath, D., Wedemeyer, H., *J. Nuc. Mater.*, 106 (1982) 191-198

ⁱⁱ Karsten, G., *J. Nuc. Mater.*, 106 (1982) 165-17

ⁱⁱⁱ Weidinger, H., Assmann, H., Holzer, R., Raab, K., *Proc. Intern. Symp. on Fabrication of Water Reactor Fuel Elements*, Prague, IAEA-SM-233/17, (1978)

^{iv} Assmann, H., Mathieu, V., Presented at 78th Annual Meeting, Am. Ceram. Soc., Cincinnati, AED- Conf-76- I 94-007, (1976)

^v Atlas, Y., et al., *J. Nuc. Mater.*, 249 (1997) 46-51

^{vi} Nuclear Fuel Conversion and Fabrication Chemistry", *Radiochemica Acta* 36, 75-84 (1984)

^{vii} HAAS, P.A., et al., "Development of Thermal Denitration to Prepare Uranium Oxide and Mixed Oxides for Nuclear Fuel Fabrication," ORNL-5735, Oak Ridge National Laboratory, Oak Ridge, TN (1981)

^{viii} Krigens, A., ARH-724, Atlantic Richfield Hanford Co., Richland, Wash., (1968)

^{ix} Hoekstra, H.R., and S. Siegel, *J. Inorg. Nucl. Chem.*, 18, (1961), 154-165